Cell Proliferation

Cell Prolif., 2010, **43**, 195–206 doi: 10.1111/j.1365-2184.2010.00669.x

Differences between karyotypically normal and abnormal human embryonic stem cells

S. Yang[1], G. Lin, Y.-Q. Tan, L.-Y. Deng, D. Yuan and G.-X. Lu

Institute of Reproductive and Stem Cell Engineering, Central South University; National Engineering Research Center of Human Stem Cells, Changsha, P. R. China

Received 15 *June* 2009; *revision accepted* 11 *July* 2009

Abstract

Objectives: To compare different biological characteristics of human embryonic stem cells (HESCs) between those with normal and those with abnormal karyotype.

Materials and methods: Culture-adapted HESCs (*ch*HES-3) with abnormal karyotype were compared with karyotypically normal cells, with regard to pluripotency and differentiation capacity, ultrastructure, growth characteristics, gene expression profiles and signalling pathways.

Results: We found a new abnormal karyotype of HESCs. We observed that *ch*HES-3 cells with normal and abnormal karyotypes shared similarities in expression markers of pluripotency; however, karyotypically abnormal *ch*HES-3 cells had a tendency for differentiation towards ectoderm lineages and were easily maintained in suboptimal culturing conditions. Abnormal *ch*HES-3 cells displayed relatively mature cell organelles compared to normal cells, and karyotypically abnormal *ch*HES-3 cells had increased survival and population growth. Genes related to cell proliferation and apoptosis were up-regulated, but genes associated with genetic instability (*p53*, *Rb*, *BRCA1*) were down-regulated in the karyotypically abnormal cells.

Conclusion: Karyotypically abnormal *ch*HES-3 cells had a more developed capacity for proliferation, resistance to apoptosis and less genetic stability compared to normal *ch*HES-3 cells and may be an excellent model for studying and characterizing initial stages that determine transition of embryonic stem cells into cancer stem cells.

Correspondence: G.-X. Lu, Institute of Reproductive and Stem Cell Engineering, Central South University; National Engineering Research Center of Human Stem Cells, Changsha, P. R. China. Tel.: +86-731-4805319; Fax: +86-731-4497661; E-mail: lugxdirector@yahoo.com.cn

[1]Present address: Human & Molecular Genetics Center, Medical College of Wisconsin, 8701 Watertown Plank Road, Milwaukee, WI 53226, USA.

Introduction

Human embryonic stem cells (HESCs) are well known to have the ability to proliferate indefinitely and to differentiate into all cell types. They are considered to be the most important 'seed' cells in cell and tissue engineering and regenerative medicine (1). One possible concern regarding use of HESCs as therapeutic tools *in vivo* is the possible risk of chromosomal variation and/or even tumour formation during long-term culture. Several studies have reported abnormal features appearing in culture-adapted HESCs including karyotypic changes (2–4), differential gene expression profiles of karyotypically abnormal HESCs (5), and that genetic changes of culture-adapted HESCs can increase their capacity for cell proliferation (6). Specific molecular markers such as CD30 confer HESCs with more pronounced resistance to apoptosis (7), whereas Enver *et al.* described the hierarchy in cell differentiation in culture-adapted HESCs and found alterations in balance between self-renewal and differentiation in culture-adapted cells (8). As the balance between self-renewal and differentiation is an essential feature of cancer cells, the mechanisms of culture adaptation may mirror those of oncogenesis and tumour progression. However, these studies only showed that HESCs might follow stages of adaptation, which could lead to tumourigenesis. To date, there have been no studies to demonstrate that karyotypic changes of culture-adapted HESCs parallel potential tumourigenic events. Thus, it is essential that the initial stages in karyotypic change in HESCs are observed and documented to determine any tumourigenic characteristics.

To explore initiation of tumourigenic characteristics underlying karyotype change, karyotypically normal and karyotypically abnormal *ch*HES-3 cells were compared.

Similarities and differences between the two cell types were assessed when cells were grown under similar controlled conditions. In addition to some characteristic similarities, differences existed as expected in their differentiation capacity *in vitro*, ultrastructure, growth characteristics, cell cycle distribution, apoptosis, self-renewal capacity and gene expression. These differences were consistent across other normal HESCs (*ch*HES-20) suggesting that fundamental differences between normal and adapted HESCs exist and that these changes may represent initiation of tumourigenic characteristics of culture-adapted HESCs.

Materials and methods

Culturing of human embryonic stem cell line chHES-3

*ch*HES-3 cells were isolated by immunosurgery and cultured in serum-free K-SR medium, containing Knockout DMEM (Gibco-BRL, Rockville, MD, USA) supplemented with 15% serum replacement (Gibco-BRL, Gaithersburg, MD, USA), 0.1 mM β-mercaptoethanol (Sigma, St Louis, Mo, USA), 1% non-essential amino acids (Gibco-BRL, Rockville, MD, USA), 2 mM L-glutamine (Gibco-BRL, Carlsbad, CA, USA), 50 U/ml penicillin (Sigma), 50 μg/ml streptomycin (Sigma) and 4 ng/ml human recombinant basic fibroblast growth factor (Gibco-BRL, Bethesda, MD, USA). *ch*HES-3 cells were initially propagated on mitomycin-C-inactivated mouse embryonic fibroblasts (mEFs) derived from inbred Kunming White mice at 12.5 days gestation, at high density of 6–7 × 10^4 cells/cm^2. Every 6–7 days, the cells were passaged using mechanical dissection or a combination of 200 U/ml collagenase IV digestion (Gibco-BRL, Rockville, MD, USA) followed by mechanical slicing.

chHES-3 cell specific marker detection

Cells were fixed in ethanol for detection of surface markers. Monoclonal primary antibodies against SSEA-1, SSEA-4, TRA-1-81 and TRA-1-60 were used and localized using rabbit anti-mouse immunoglobulins conjugated to fluorescein isothiocyanate and stained using the ES Marker Sample kit (Chemicon, Temecula, CA, USA). Oct-4 staining was performed according to the manufacturer protocol (Santa Cruz Biotechnology, Santa Cruz, CA, USA). Alkaline phosphatase (AKP) activity was detected as described previously (9).

Karyotype analysis

Culture-adapted ES cells were cultured overnight in HES medium containing 0.06 μg/ml Colcemid (Sigma). After washing three times in PBS, the cells were incubated in HES medium containing 0.05% trypsin and 0.53 mM EDTA (Gibco-BRL) at 37 °C for 10 min and harvested using standard procedures, followed by standard G-banding for karyotyping.

Electron microscopy

The normal and abnormal karyotype embryonic stem cells were grown on an MEF feeder cell layer. Once they had formed sizable colonies, they were fixed in 5% glutaraldehyde for 3 h and processed for electron microscopy. They were post-fixed in osmium tetroxide and embedded in plastic resin; then they were formed into semi-thin section of 1 μm and stained with toluidine blue. In addition, thin sections were prepared for electron microscopy according to a standard protocol.

Colony formation experiment

The karyotypically normal and abnormal cells were cultured in ES medium for 4 days then digested to single cells. After counting, the single cells (2000/well) were seeded into six-well plates containing inactivated mouse embryonic feeder cells. After 2 weeks, colonies were fixed and stained with AKP; positive AKP populations were considered to be single colonies.

Cell proliferation

The cells from both karyotypically normal and abnormal *ch*HES-3 cells were detached using trypsin and counted using a haemocytometer. Then single cells were seeded at 2 × 10^5/25 cm^2 on feeder layers. After culturing for 4 and 6 days in ES medium, cells were harvested and counted.

Basic fibroblast growth factor dependence

Karyotypically normal and abnormal *ch*HES-3 cells were seeded into six-well plates in ES medium [4 ng/ml basic fibroblast growth factor (bFGF)]. Undifferentiated cells were then selected for experiments after attachment for 1 day. They were washed twice in PBS before the undifferentiated cells were cultured in bFGF-free ES medium. After 4 days, numbers of undifferentiated clones and ratios of undifferentiation in each cell were calculated, harvesting wells in triplicate.

Microarray data analysis

Total RNA was extracted from cells using RNasy Mini Kit (Qiagen, Valencia, CA, USA). One microgram of

total RNA was primed with 100 ng of Oligo dT-T7 primer and reverse transcribed with Superscript II (Invitrogen, Carlsbad, CA, USA). Second strand was synthesized and double strand cDNA purified using the DNA Clean and Concentrator kit (Zymo Research, Orange, CA, USA). The *in vitro* transcription reaction was incubated for 9 h with T7 RNA polymerase. First round aRNA was purified using RNeasy Mini Kit (Qiagen, Valencia, CA, USA) and second round amplification was performed in a similar way to first round, but with 100 ng of aRNA and 500 ng random hexamers. Following second round dscDNA, the ENZO BioArray High-Yield RNA Transcript Labelling Kit (Affymetrix, Santa Clara, CA, USA) was used to incorporate biotin-labelled nucleotides, and then RNA was purified using RNeasy kit. Fragmentation was completed according to the standard protocol (Affymetrix). Prior to hybridization on the GeneChip array, a test array of housekeeping controls was analysed to determine sample suitability for GeneChip arrays. Hybridized arrays were subsequently scanned for data analysis (detailed RNA amplification protocol available upon request). Rehybridization was completed and removed from pre-hybridization buffer; gene chips were filled with 200 ml of hybridization mixture and incubated for 16 h at 45 °C at 60 rpm. The hybridization mixture was removed and stored at −70 °C. Each chip was filled with 250 ml of non-stringent wash buffer (6X SSPE, 0.01% Tween-20) and the signal was amplified by additional treatment with goat-IgG antibody (0.1 mg/ml) and biotinylated antibody (3 mg/ml) for second staining with SAPE. Chips were scanned using an Affymetrix Scanner 3000 (Affymetrix) and gene expression signal was collected using Affymetrix GCOS V1.1.1 software.

Polymerase chain reaction and real-time PCR analysis

A total of 1×10^6 *ch*HES-3 cells was collected and total RNA extracted using Trizol and RNAeasy RNA Cleanup kit. RNA was treated with RNase-free DNase for 20 min (Roche, Basel, Switzerland) at room temperature. A 4 μl aliquot of total RNA was reverse-transcribed in a thermocycler using virus reverse transcriptase with random primers according to the manufacturer's protocol (Sigma). Gene-specific primer (see Tables S1 and S2) sets were designed and optimized. Real-time polymerase chain reaction (PCR) was performed using Lightcycler Faststart DNA Sybr Green I kit according to the protocol provided. To determine specificity of amplified products, a melting curve analysis was performed. No amplification of non-specific products was observed. Cycle threshold (C_t) values were obtained for the tested genes and relative change was calculated in normal cell versus abnormal samples using the $2^{-\Delta\Delta Ct}$ method as described (10), and 95% confidence intervals. Experiments were repeated three times.

Analysis of apoptosis

Apoptotic cells were examined using the Annexin V-FITC kit (Bender MedSystems, Vienna, Austria) according to manufacturer's instructions.

Western blot analysis

Protein extracts from 5×10^6 *ch*HES-3 cells were separated by classical methods and transferred on to nitrocellulose membranes. Membranes were blocked with 5% dry milk and probed using monoclonal antibody to p53 (pAb1801; Santa Cruz Biotechnology). The filter was then incubated in horseradish peroxidase-conjugated secondary antibody and developed with enhanced chemiluminescence PLUS reagent from Amersham (Piscataway, NJ, USA). To ensure that the amount of protein in each lane was comparable, the filter was stripped and probed with rabbit polyclonal antibody to β-actin (Santa Cruz Biotechnology).

Results

Karyotype changes and characteristics of chHES-3 cells

Our established *ch*HES-3 cell line, was cultured in serum-free medium on embryonic fibroblast cells isolated from Chinese Kun-Min White mouse at a density of $6–7 \times 10^4$ cells/cm^2. At this density, *ch*HES-3 colonies exhibited compact appearance and showed spontaneous progressive differentiation at their periphery from day 3 to day 7 after passaging. During long-term culture, several growth crises occurred due to intensive differentiation. Cells rescued from undifferentiated regions of the dish could be split again and exhibited adaptive growth advantage. During routine follow-up examination of karyotype once in every five passages, the cells exhibited normal karyotype at passage 19 (Fig. 1a). By passage 29, among all analysed 50 metaphases, there were 23 metaphases with karyotype of 46, XX dup (1p32–1p36). At passage 34, the karyotype [46, XX dup (1p32–1p36)] was observed in all 50 analysed metaphases (Fig. 1b). Karyotypically abnormal cells expressed the predicted HESC pluripotency markers *SSEA-4, SSEA-3, TRA-1-81, TRA-1-60* and *Oct3/4* (Fig. 1c) (part of these results had been published in *Gene, Chromosome and Cancer*). RT-PCR was performed to identify genes associated with differentiation and pluripotency, such as *NANOG, TERT, THY1, PECAM1, CD34, T* (brachyury)*, AFP, CDH5, FLT1, NES* (nestin)*, TF and TNFRSF8.* Their expression profiles

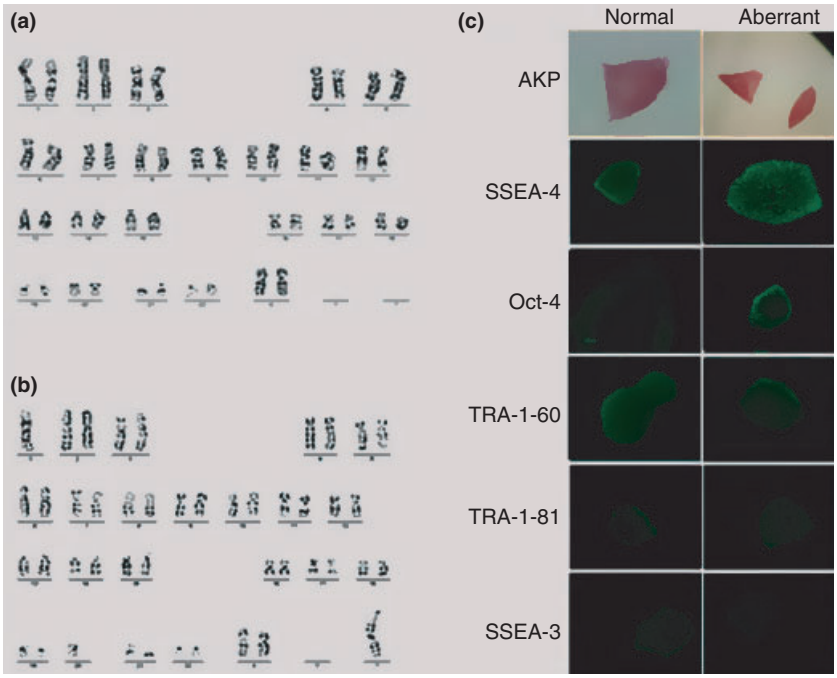

Figure 1. Characteristics of karyotypically abnormal *ch*HES-3 cells. (a) Normal karyotype of 46, XX at passage 19. (b) Abnormal karyotype of 46, XX, dup (1) (p32p36) at passage 34. (c) Karyotypically abnormal and normal *ch*HES-3 cell colonies stained positive for AKP, SSEA-4, OCT-4, TRA-1-60 and TRA-1-81 expression and negative for SSEA-1.

(Table 1) suggested that karyotypically abnormal *ch*HES-3 cells were sufficiently pluripotent to differentiate into all three germ cells.

In vitro differentiation of chHES-3 cells with normal and abnormal karyotypes

The *ch*HES-3 cells with normal (P27) and abnormal (P38) karyotype developed into embryonic bodies (EB) in suspension culture after 7 days (Fig. 2a). Seven-day-old EBs were replated on dishes and cultured in the same medium; various cell types appeared in the outgrowth after 15 days. Immunocytochemical analysis using antibodies against β-tubulin (ectoderm), smooth muscle antigen (mesoderm) and alpha-fetoprotein (endoderm) showed differentiation into all three embryonic germ layers by both normal and abnormal-karyotype cells (Fig. 2b–d). Samples were removed from the cultures at 0, 1, 3 and 7 days of differentiation, and markers indicative of pluripotency (*NANOG*) and differentiation to endoderm (*AFP*), mesoderm (*KDR*) and ectoderm (*PAX6*) were assayed using real-time PCR. Expression of *NANOG* decreased dramatically in 1 day, specially in the normal cells (Fig. 3a). *AFP* expression increased significantly after 3 days differentiation of the normal cells, but not in aberrant-karyotype cells (Fig. 3b). Expression of the mesoderm marker, *KDR*, increased for 3 days, then decreased after 7 days, specially in karyotypically abnormal cells (Fig. 3c). Finally, *PAX6* (ectoderm marker) expression increased significantly in 3 days differentiation in both types of HES cells, but increased more rapidly in the abnormal ones than in normal ones (Fig. 3d). Interestingly, this tendency for ectodermal lineage expression was also observed during suboptimal culturing in bFGF-free

Table 1. Analysis of markers

Marker	Normal	Abnormal	Normal EB	Abnormal EB
Oct-4	+	+	Nt	Nt
Tra 1-60	+	+	Nt	Nt
Tra 1-81	+	+	Nt	Nt
SSEA-4	+	+	Nt	Nt
SSEA1	–	+	Nt	Nt
CD9	+	+	Nt	Nt
Vimentin	–	+	Nt	Nt
CD133	–	+	+	+
Using RT-PCR				
Oct-4	+	+	+	+
hTERT	+	+	+	+
Nanog	+	+	+	+
CD90	+	+	+	+
CD31	–	–	+	+
CD34	–	+	+	+
Brachyury	–	+	+	–
VE-cadherin	–	+	+	–
AFP	–	–	+	–
Flt-1	–	+	+	+
Nestin	+	+	+	+
Transferrin	–	+	+	+
Beta-actin	+	+	+	+

Tested by immunohistochemistry (IHC) or RT-PCR.
Nt, not tested; Normal, karyotypically normal *ch*HES-3 cells at P27; Aberrant, karyotypically abnormal chHES-3 cells at P38; Normal EB, EB from karyotypically normal *ch*HES-3 cells at P27; Aberrant EB, EB from karyotypically abnormal *ch*HES-3 cells at P38.

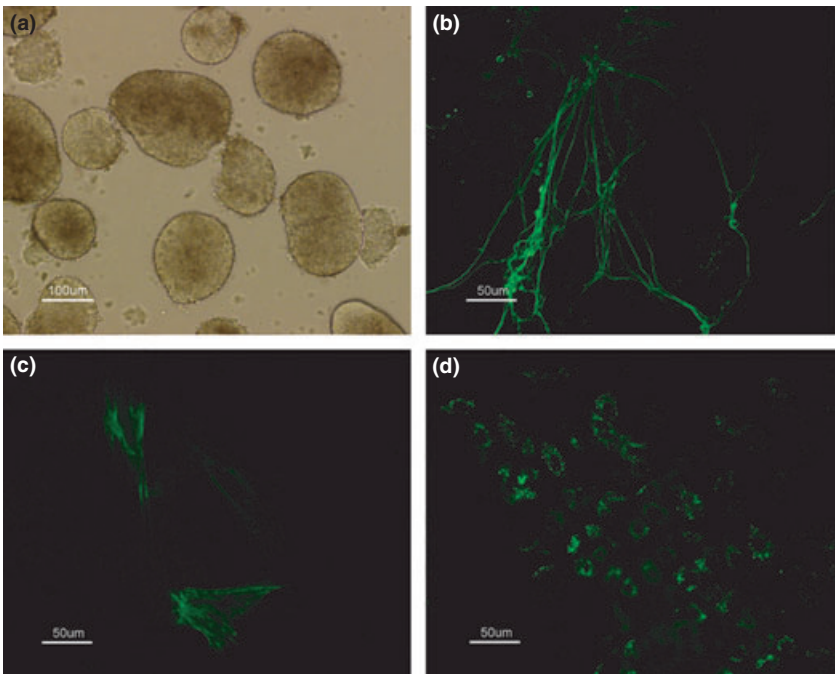

Figure 2. Differentiation of karyotypically abnormal *ch*HES-3 cells *in vitro*. (a) Embryoid body derived from karyotypically abnormal *ch*HES-3 cells. Results of immunocytochemical analysis, positive for ß-tubulin (b), SMA (c) and AFP (d).

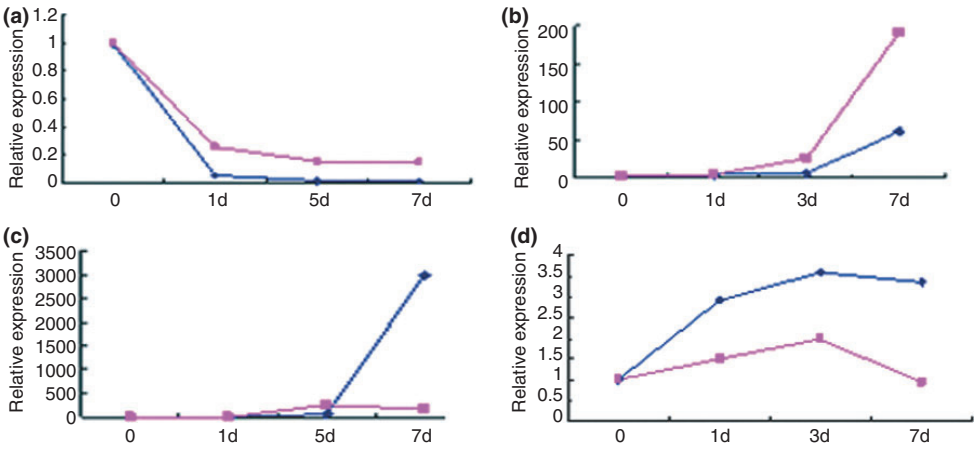

Figure 3. *In vitro* differentiation of *ch*HES-3 cells with normal and abnormal karyotypes. (a) Nanog, a marker of undifferentiated ES cells, (b) AFP, endoderm marker, (c) Pax6, ectoderm marker, and (d) KDR, mesoderm marker were assayed at each time point over a period of 7 days. Expression levels of the markers are shown relative to normal *ch*HES-3 cells on day 0 (Blue: The normal *ch*HES-3, red: The karyotypically abnormal *ch*HES-3).

culture medium on high-density feeders. Karyotypically abnormal cells were easily maintained in an undifferentiation state compared to normal cells (Fig. 4a,b). However, the karyotypically abnormal cells exhibited a tendency for spontaneous differentiation into primary nerve cells, an ectodermal lineage. In contrast, cells near the border of the karyotypically normal colonies became linear and radiate, showing fibroblast-like cell morphology (Fig. 4c,d). Expression data and culture observations suggest that although both normal and abnormal-karyotype *ch*HES-3 cells were capable of differentiating into cells of all three embryonic germ-layers after embryoid body formation, abnormal-karyotype cells tended to commit to ectoderm.

Ultrastructure of karyotypically abnormal chHES-3 cells

Compared to karyotypically normal *ch*HES-3 cells, karyotypically abnormal ones had fewer apoptotic cells, specially those close to the edge of colonies (not shown). In addition, fewer autophagosomes (found in almost a quarter of all of karyotypically normal *ch*HES-3 cells),

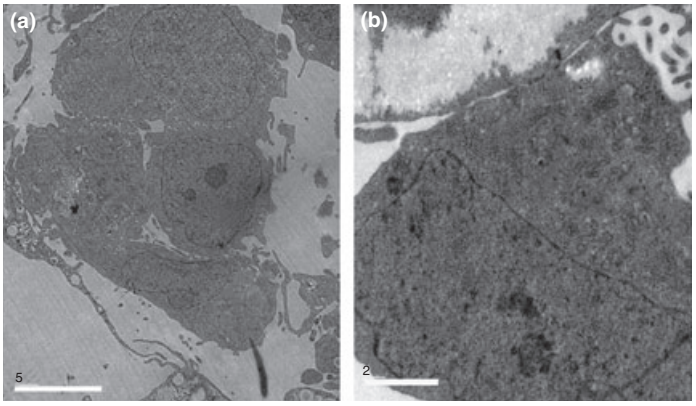

Figure 4. Ultrastructure of *ch*HES-3 cells with normal and abnormal karyotype. (a) Ultrastructure of karyotypically abnormal *ch*HES-3 cells shows them having high nucleus-to-cytoplasm ratio, while few cell organelles in the cytoplasm. (b) Electron-dense lysosomal structures, mitochondria and Golgi bodies well developed in the cytoplasm.

were visible (not shown). However, electron-dense lysosomal structures, mitochondria, Golgi bodies and endoplasmic reticular apparatus in cytoplasm of all appeared more developed in karyotypically abnormal cells (Fig. 5a,b).

Population growth characteristics of karyotypically normal and abnormal chHES-3 cells in culture

Under abnormal ES culturing conditions (high density feeders, no bFGF), karyotypically abnormal *ch*HES-3 cells had substantially greater population growth rates and single colony formation efficiencies than normal *ch*HES-3 cells (Fig. 6a,b). In addition as predicted, karyotypically normal cells were more susceptible to differentiation and death under these conditions; after 5 days in culture, percentage of undifferentiated colonies was only 32 ± 1.60% (most were floating dead cells). In contrast, the percentage of undifferentiated colonies formed by karyotypically abnormal cells 5 days after passaging was 87 ± 2.4%, indicating that karyotypically abnormal cells resisted not only differentiation, but also death (most cells were viable, data not shown) (Fig. 6c).

Indeed, comparison of spontaneous apoptosis between karyotypically normal and abnormal cells revealed that in normal *ch*HES-3 cells, the percentage of spontaneous apoptotosis was 10.7 ± 0.45% (mean values of three experiments), while karyotypically abnormal cells at passages 38, 39 and 40 showed apoptotic rates of 4.7%, 4.2% and 3.0% respectively (mean value 3.96 ± 0.87%) (Fig. 6d).

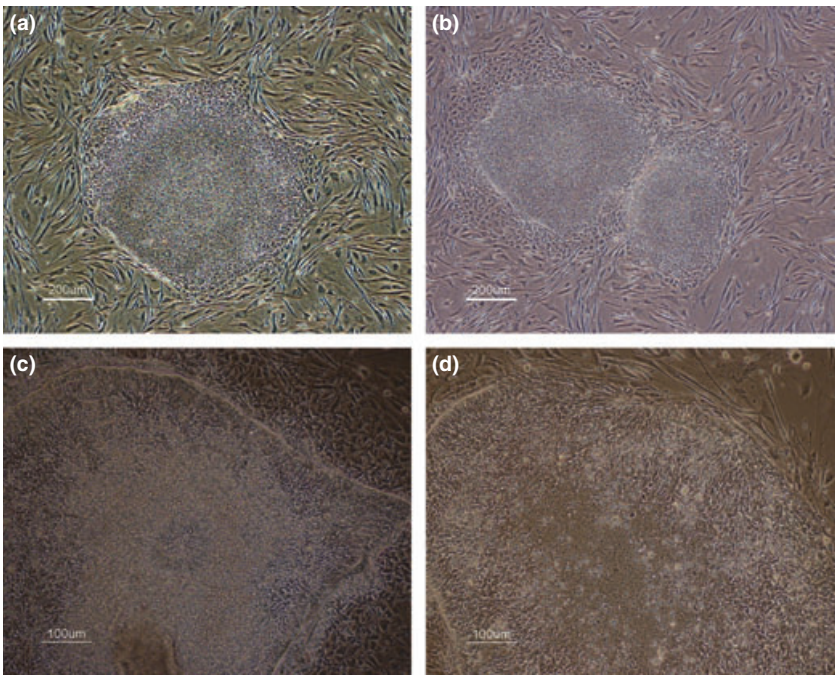

Figure 5. Growth morphology of *ch*HES-3 cells with normal and abnormal karyotype. (a) No differentiation at the periphery of colony in karyotypically abnormal *ch*HES-3 cells. (b) Obvious differentiation in normal *ch*HES-3 cells. (c) karyotypically abnormal *ch*HES-3 cells exhibiting capacity for extensive differentiation into primary nerve cells. (d) In karyotypically normal *ch*HES-3 cells, some at borders of colonies become linear and radiate, showing fibroblast-like cell morphology.

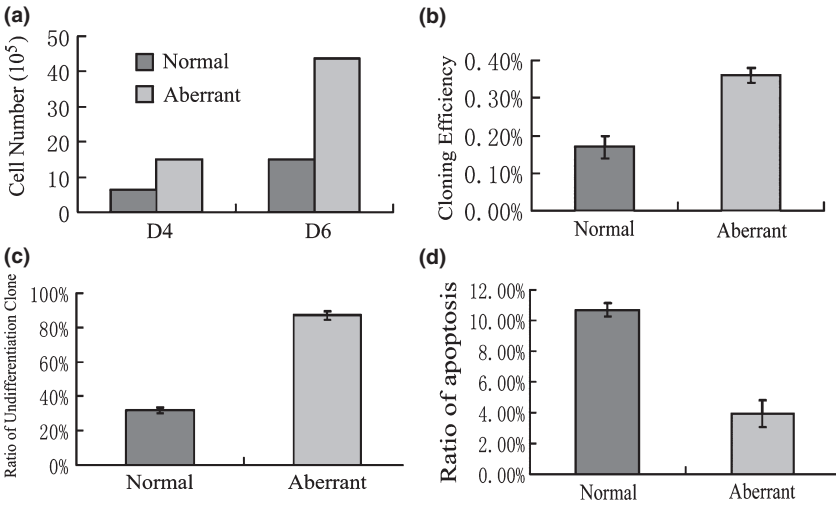

Figure 6. Growth characteristics of *ch*HES-3 cells with normal and abnormal karyotype. (a) Karyotypically aberrant *ch*HES-3 cells had substantially greater population growth rates than normal *ch*HES-3 cells. (b) Karyotypically aberrant *ch*HES-3 cells had higher single colony efficiencies. (c) In bFGF-free medium, karyotypically aberrant *ch*HES-3 cells were susceptible to maintainance. (d) Apoptotic ratio in karyotypically normal (10.7 ± 0.45%) and abnormal *ch*HES-3 cells (3.96 ± 0.87%).

Together, increase in population growth rate and decrease in rate of spontaneous differentiation and apoptosis suggest that the karyotypically abnormal cells, which arose after long-term culturing, share properties with pre-malignant tumourigenic cells.

Up-regulation oncogenes in duplication regions

The 1p32–1p36 duplication spontaneously arising in karyotypically abnormal *ch*HES-3 cells suggests that dosage variation of the genome might confer these abnormal cells with higher potential for cell proliferation (2, 11) and could be an important event in malignant cell transition and genomic instability. Accordingly, we analysed expression of known oncogenes in the region, including *HKR3, LCK, MPL, MYCL1, BLF, TAL1* and *JUN*, using semi-quantitative PCR. Of these, expression levels of *HKR3, LCK, JUN* and *TAL1* were up-regulated in karyotypically abnormal *ch*HES-3 cells (Fig. S1).

Chromosomal distribution of differentially expressed genes between karyotypically abnormal and normal chHES-3 cells

In order to determine whether expression of genes in karyotypically abnormal *ch*HES-3 cells may be associated with non-random genomic amplification in certain hot-spot areas, we performed gene chip (GSM172579 and GSM172580) analysis on karyotypically normal and abnormal cells (Fig. S2) and mapped chromosomal locations of differentially expressed genes. In comparison to normal *ch*HES-3 cells, down-regulated genes in karyotypically abnormal ones were distributed randomly across all chromosomes (data not shown), while most up-regulated genes were clustered in the duplication region of 1p32-36 (Fig. 7a). Interestingly, after normalizing for the length of each chromosome, highly expressed genes in karyotypically abnormal *ch*HES-3 cells revealed that there was over-representation of up-regulated genes on chromosomes 1 and 17 (Fig. 7b and Table 2). However, adjusting for gene number of each chromosome, using UniGene clusters (Build 34, version 3) showed that there was over-representation on chromosome 1 (Fig. 7c).

Expression of genes related to apoptosis in karyotypically normal and karyotypically abnormal chHES-3 cells

Comparing gene profiles between karyotypically normal and karyotypically abnormal *ch*HES-3 cells, 35 genes related to apoptosis were found to be significantly differentially expressed. Among 11 genes which were up-regulated, *BNIP3*, *BIRC5*, *IER3*, *NME5*, *MIF* and *BNIP3L* were anti-apoptotic, hence negatively regulated apoptosis. Among 24 genes which were down-regulated, *TNFRSF19*, *CFLAR*, *F2R*, *BCLAF1*, *CASP7*, *PLAGL1*, *TIA1*, *CUL2*, *PAWR* and *BAX* expression induces apoptosis and positively regulating it. However, the functions of eight further genes related to apoptosis remain unclear (Table 3). To verify results of microarray analysis, *CASP3*, *CUL2, EP300* and *TP53* were confirmed using real-time PCR (Fig. 8a).

Expression of genes related to cell proliferation

Given the differences observed by cell population growth characteristics, it was reasoned that karyotypically normal and abnormal *ch*HES-3 cells would display additional differences in gene expression related to cell proliferation. Indeed, gene chip analysis revealed that among the differentially expressed genes, almost all including *CDC25A*,

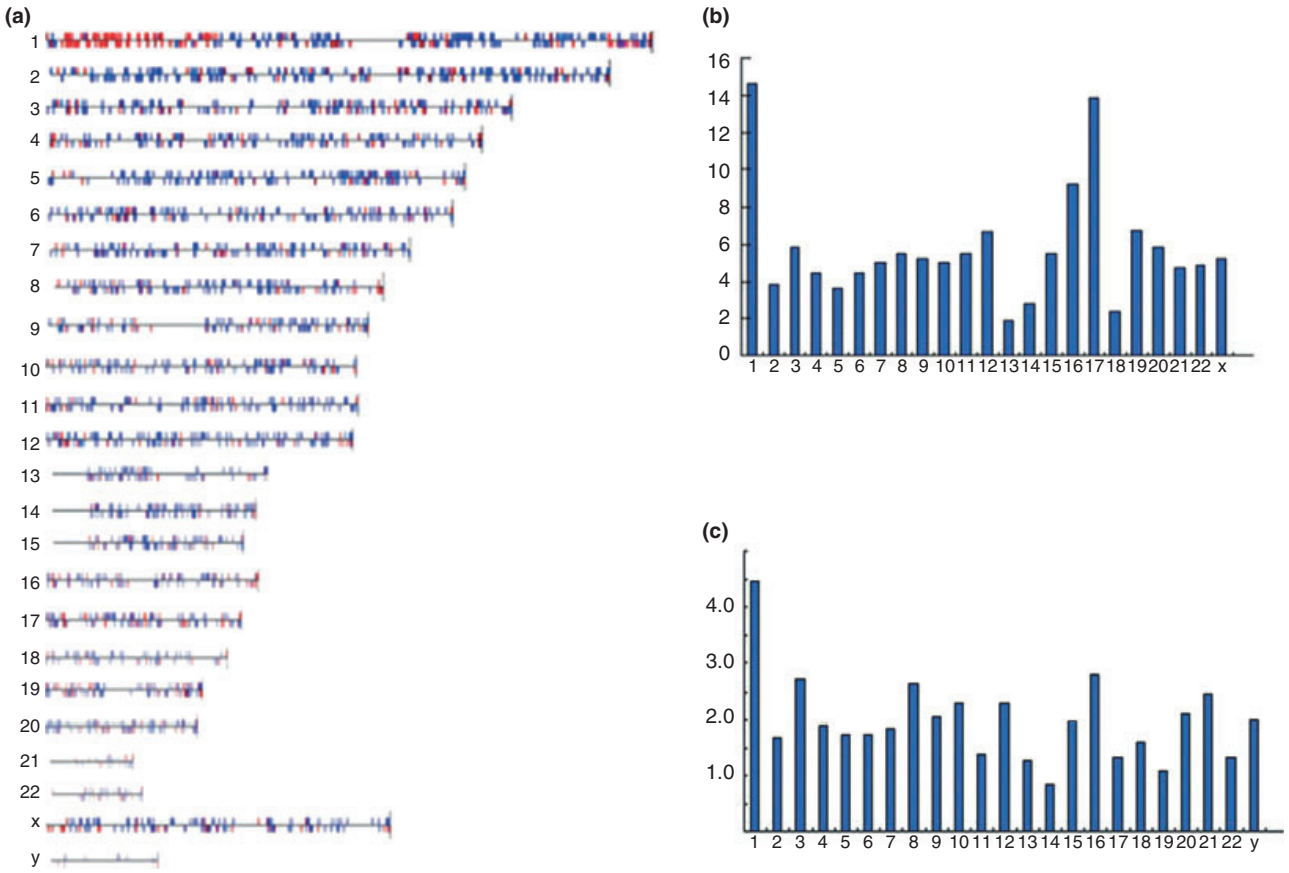

Figure 7. Chromosomal distribution of up-regulated genes normalized by gene number and chromosome size. (a) Up-regulated genes relatively clustered on duplication region of chromosome 1. (b) Distribution of up-regulated genes per chromosome, normalized by size of chromosomes on each chromosome. Chromosome size acquired from Ensemble 7. (c) Distribution per chromosome normalized by number of UniGene clusters per chromosome. Number of UniGene clusters (Build 34, version 3) from NCBI.8.

SMC1A, *SMAD4, SKP2*, *RB1*, *PRKDC*, *PLK1*, *MCM4*, *MCM2*, *HDAC6*, *ESPL1*, *E2F5*, *DTX4*, *CHEK1*, *CDH1*, *CDC7*, *CDC14A*, *CCNE2*, *CCND2*, *BUB3*, *BUB1*, *ATM* and *ABL1* were down-regulated; only *HDAC1*, *CDC20*, *MAD2L2*, *PTTG1*, *CCNA1* and *HDAC7A* were up-regulated. Interestingly, *HDAC1*, *CDC20* and *MAD2L2* all mapped to the region of 1p32–36. Results are summarized in Table S3. Differential expression of some genes (*BUB1, SMAD4, RB1* and *CDC20*) was confirmed using real-time PCR (Fig. 8b).

Analysis of cell cycle checkpoint signalling pathways

To further address the molecular mechanism of abnormal *ch*HES-3 cells, we looked more closely at cell cycle signalling pathways. G_1 to S cell cycle transformation-related genes including *CDC2*, *TGFB1*, *MAD2L2*, *TRAF4* and *NACA*, were up-regulated in karyotypically abnormal *ch*HES-3 cells, while cell cycle arrest-related genes including *GAS1*, *SESN3*, *PLAGL1* and *CUL2* were down-regulated except for *MACF1*, which was up-regulated. In addition, four cyclin-dependent kinase inhibitor genes (*CDKN1A, CDKN1B, CDKN2A* and *CDKN2B*) were down-regulated. Within cell cycle checkpoint gene pathways, *RB1, ATM, CHEK1, CDC25A*, *WEE1, BRCA1* and *TP53* were all down-regulated, while *CDKN2A* was equally expressed in karyotypically normal and abnormal cells. Decreased expression of *TP53*, *RB1* and *BRCA1* in the karyotypically abnormal *ch*HES-3 cells was confirmed using real-time PCR (Fig. 8c). In addition, down-regulation of *TP53* protein in karyotypically abnormal cells was shown by Western blot analysis (Fig. S3).

Discussion

Several previous reports have indicated that the karyotype of HESCs may change during long-term culture, usually acquiring an additional copy of chromosomes 1,

Table 2. Chromosomal distribution of the over-expression genes in karyotypically abnormal *ch*HES-3 cells by normalizing with the length and numbers (UniGene clusters) of each chromosome

chr	The number of up-regulated genes	The relative length of the chromosome	The normalized number of gene expression by chromosome size	The number of genes per chromosome	The normalized ratios of gene expression by number of Unigene clusters per chromosome
1	124	8.44	14.69	2776	0.0447
2	31	8.02	3.87	1866	0.0166
3	40	6.83	5.86	1473	0.0272
4	28	6.30	4.44	1164	0.0190
5	22	6.08	3.62	1281	0.0172
6	26	5.90	4.41	1528	0.0170
7	27	5.36	5.04	1474	0.0183
8	27	4.93	5.48	1025	0.0263
9	25	4.80	5.21	1207	0.0207
10	25	4.95	5.05	1094	0.0229
11	25	4.61	5.42	1841	0.0136
12	31	4.66	6.65	1355	0.0229
13	7	3.74	1.87	556	0.0126
14	10	3.56	2.81	1220	0.0082
15	19	3.46	5.49	961	0.0198
16	31	3.36	9.22	1108	0.0280
17	45	3.25	13.84	1442	0.0132
18	7	2.93	2.39	438	0.0160
19	18	2.67	6.74	1624	0.0110
20	15	2.56	5.86	717	0.0209
21	9	1.90	4.74	367	0.0245
22	10	2.04	4.90	756	0.0132
X	27	5.12	5.27	1344	0.0200

12, 17, or X (12–15). These changes are similar to those found in germ cell tumours such as malignant embryonal carcinoma (16,17). Karyotype, 46, XX dup (1p32–1p36) found in this study was different from those previously reported in HESCs. Interestingly, 1p32 and 1p36 are common sites of fragility, which has been shown often to be involved in chromosomal rearrangements arising in HESC (18).

Karyotype changes are known to affect the function of ES cells (19) and likewise, our results have shown that karyotypically abnormal *ch*HES-3 cells can be maintained easily in suboptimal conditions, had a higher ratio of single clone formation and lower-bFGF dependence *in vitro*, compared to karyotypically normal ones, indicating that the karyotypically abnormal *ch*HES-3 cells had more self-renewal capacity. There were some disparities in differentiation between karyotypically normal and abnormal *ch*HES-3 cells *in vitro* as abnormal ones easily differentiated into ectoderm, but normal *ch*HES-3 cells tended to differentiate into mesoderm and endoderm.

Identifying amplified genes in duplication regions of karyotypically abnormal *ch*HES-3 cells responsible for biological characteristics remains a challenge. Because some oncogenes, such as *MYC*, play an important role in maintaining the ES state (20), we examined expression of oncogenes located in the duplication region and found that, among genes up-regulated in karyotypically abnormal *ch*HES-3 cells, *HKR3, LCK, JUN* and *TAL1* are new promising candidates for ES state maintenance and induced pluripotent stem cell formation.

Characteristics of some visible structures in living human ES cell colonies are reported here. Compared to karyotypically normal *ch*HES-3 cells, karyotypically abnormal ones had higher nucleus⁄cytoplasm ratio and cytoplasmic components tended to be larger and more complex. In karyotypically abnormal *ch*HES-3 cells, organelles related to energy metabolism in the cytoplasm, such as lysosomal structures, mitochondria and Golgi apparatus were more developed. It seems that a switch in energy metabolism occurs from one based principally on aerobic respiration to the other based on both oxidative phosphorylation and aerobic glycolysis, as reported previously (21,22), indicating that karyotypically aberrant *ch*HES-3 cells had higher energy metabolism, required for cell proliferation. These findings might hold the key to an explanation that karyotypically abnormal *ch*HES-3 cells

Table 3. The expression of differentiation genes related to the apoptosis

Gene	Change	Chromosomal location	Accession	Function
TNFRSF19	D	chr13q12.11-q12.3	BF432648	Positive
FKSG2	D	chr8p11.2	NM_021631	Negative
UBE1C	D	chr3p24.3-p13	BM353142	Regulation of apoptosis
CFLAR	D	chr2q33-q34	AF015451	Positive
F2R	D	chr5q13	NM_001992	Positive
IGFBP3	D	chr7p13-p12	M31159	Apoptosis
BCLAF1	D	chr6q22-q23	AA740754	Positive
TRAF4	D	chr17q11-q12	BF000155	Regulation of apoptosis
CASP7	D	chr10q25	NM_001227	Positive
MCL1	D	chr1q21	NM_021960	Negative
PLAGL1	D	chr6q24-q25	NM_002656	Positive
TNFRSF18	D	chr1p36.3	AF117297	Negative
TP53INP1	D	chr8q22	AW341649	Apoptosis
TIA1	D	chr2p13	NM_022037	Positive
SOCS2	D	chr12q	NM_003877	Negative
CUL2	D	chr10p11.21	U83410	Positive
BNIP2	D	chr15q22.2	BC002461	Negative
MAGI3	D	chr1p12-p11.2	AI692181	Apoptosis
CBX4	D	chr17q25.3	AI570531	Apoptosis
CD40	D	chr20q12-q13.2	X60592	Negative
EP300	D	chr22q13.2	AV727101	Regulation of apoptosis
PAWR	D	chr12q21	NM_002583	Positive
CASP3	D	chr4q34	NM_004346	Apoptosis
BAX	D	chr19q13.3-q13.4	U19599	Positive
BNIP3	I	chr10q26.3	U15174	Negative/positive
BIRC5	I	chr17q25	BQ021146	Negative
LGALS1	I	chr22q13.1	M14087	Regulation of apoptosis
SEPT4	I	chr17q22-q23	U88870	Regulation of apoptosis
EGLN3	I	chr14q13.1	AI378406	Apoptosis
BNIP3L	I	chr8p21	AF060922	Negative/positive
IER3	I	chr6p21.3	NM_003897	Negative
NALP2	I	chr19q13.42	AF298547	Apoptosis
ITGB3BP	I	chr1p31.3	NM_014288	Positive
NME5	I	chr5q31	NM_003551	Negative
MIF	I	chr22q11.23	NM_002415	Negative

Positive, positive regulation of apoptosis; Negative, negative regulation of apoptosis.

had high proliferation aligned with energy metabolism level.

Another conceptually important question we asked is concerned with the mechanism of differential expression of so many genes in karyotypically aberrant *ch*HES-3 cells. Over-representation of transcripts may not only be a result of true functional up-regulation but also reflect gene–dosage effect caused by structural amplification (for example, duplication of parts of chromosome regions), specially when over-represented genes appeared in clusters. Chromosomal distribution of genes up-regulated in our samples revealed that this was not random. Two chromosomal regions of over-expression were 1p and 17, which have often been reported in testicular germ cell tumours (23). However, in our study, only 1p duplications were detected, thus, we conclude that expression pattern observed in karyotypically abnormal *ch*HES-3 cells is likely to be the combined result of genomic amplification and increased transcriptional activation.

In somatic cells, *P53* and *RB* signalling pathways play an important role in maintaining cell genetic stability (24). In cancer cells, these two pathways tend to be disregulated and lead to genetic instability (25,26). In previous reports, ES cells were deficient in cell cycle checkpoints (27), but here *P53* and *RB* were down-regulated in karyotypically abnormal *ch*HES-3 cells, which may affect function of the G_1 to S phase checkpoint and could result in increasing numbers of cells with aberrant genetic material entering the cell cycle. Thus, in the proliferating cell population, karyotypically abnormal *ch*HES-3 cells became dominant. Other studies have reported that *P53* inhibited self-renewal of ES cells and promoted ES cell differentiation and apoptosis (28,29). In contrast, our studies suggest that in karyotypically aberrant *ch*HES-3 cells, down-regulation

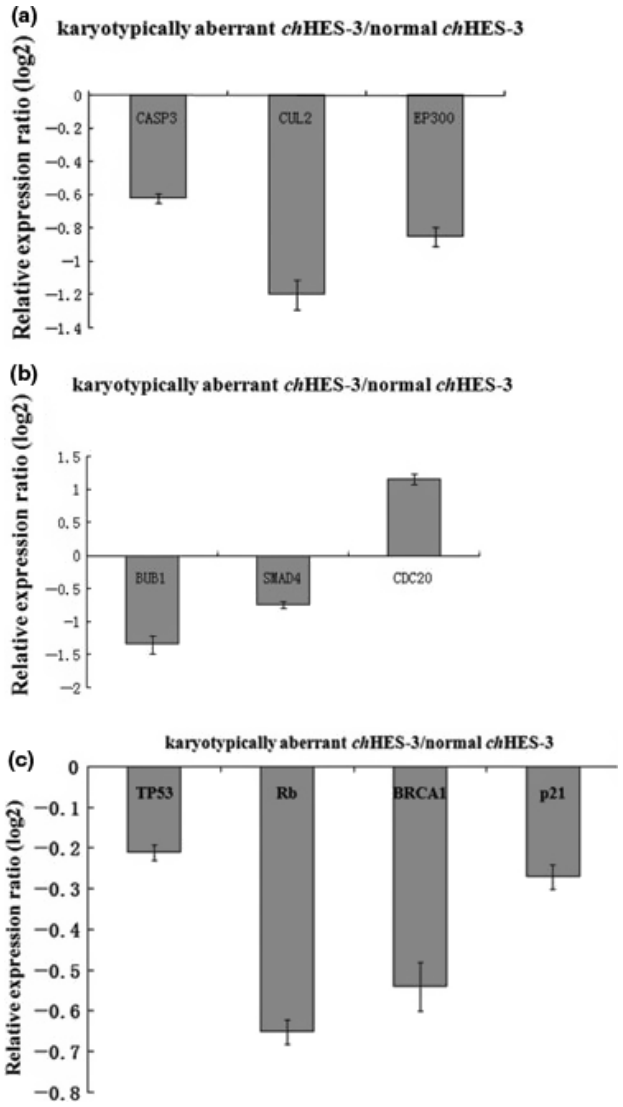

Figure 8. Relative expression level of genes between karyotypically normal and abnormal *ch*HES-3 cells. Relative expression ratio of genes related to apoptosis (a), cell proliferation (b) and genetic stability (c) in karyotypically abnormal *ch*HES-3 cells.

of *P53* enhances self-renewal, anti-differentiation and anti-apoptosis. We hypothesize that, due to down-regulation of *P53*, balance of self-renewal, differentiation and genetic stability was deregulated; karyotypically abnormal *ch*HES-3 cells had more self-renewal power, lower differentiation and weaker genetic stability.

Earlier studies of embryonal carcinoma and culture-adapted HESCs has shown that adapted HESCs have a tendency to progress towards being cancer stem cells during long-term culture (30). The mechanisms driving adaptation and selection of these variants *in vitro* might provide insight into the mechanisms underlying cancer stem cell progression (31). In the design presented in this study, deregulation of *P53* leads to progression of genetic instability, and thus tumourigenic characteristics emerged in karyotypically abnormal *ch*HES-3 cells; these with tumourigenic characteristics may represent an excellent model for exploring early events leading from embryonic stem cells to cancer stem cells.

Acknowledgements

The authors thank Associate Prof. Jozef Lazar **and** Assistant Prof. Aron Geurts for revising and editing the manuscript. This study was supported by the National Natural Science Foundation Major Program of China (No. 30030070), the Hi-Tech Research and Development of China (863 program No. 2003AA205181 and 2006AA02A102) and the National Basic Research Program of China (973 program No. 00CB 51010).

References

1 Thomson JA, Itskovitz-Eldor J, Shapiro SS, Waknitz MA, Swiergiel JJ, Marshall VS *et al.* (1998) Embryonic stem cell lines derived from human blastocysts. *Science* **282**, 1145–1147.
2 Draper JS, Smith K, Gokhale P, Moore HD, Maltby E, Johnson J *et al.* (2004) Recurrent gain of chromosomes 17q and 12 in cultured human embryonic stem cell. *Nat. Biotechnol.* **22**, 53–54.
3 Lefort N, Feyeux M, Bas C, Féraud O, Bennaceur-Griscelli A, Tachdjian G *et al.* (2008) Human embryonic stem cells reveal recurrent genomic instability at 20q11.21. *Nat. Biotechnol.* **26**, 1364–1366.
4 Spits C, Mateizel I, Geens M, Mertzanidou A, Staessen C, Vandeskelde Y *et al.* (2008) Recurrent chromosomal abnormalities in human embryonic stem cells. *Nat. Biotechnol.* **26**, 1361–1363.
5 Mitalipova MM, Rao RR, Hoyer DM, Johnson JA, Meisner LF, Jones KL *et al.* (2005) Preserving the genetic integrity of human embryonic stem cells. *Nat. Biotechnol.* **23**, 19–20.
6 Baker DE, Harrison NJ, Maltby E, Smith K, Moore HD, Shaw PJ *et al.* (2006) Adaptation to culture of human embryonic stem cells and oncogenesis in vivo. *Nat. Biotechnol.* **25**, 207–215.
7 Herszfeld D, Wolvetang E, Langton-Bunker E, Chung TL, Filipczyk AA, Houssami S *et al.* (2006) CD30 is a survival factor and a biomarker for transformed human pluripotent stem cells. *Nat. Biotechnol.* **24**, 351–357.
8 Enver T, Soneji S, Joshi C, Brown J, Iborra F, Orntoft T *et al.* (2005) Cellular differentiation hierarchies in normal and culture-adapted human embryonic stem cells. *Hum. Mol. Genet.* **14**, 3129–3140.
9 Xie CQ, Lin G, Luo KL, Luo SW, Lu GX (2004) Newly expressed proteins of mouse embryonic fibroblast irradiated to be inactive. *Biochem. Biophys. Res. Commun.* **315**, 581–588.
10 Livak KJ, Schmittgen TD (2001) Analysis of relative gene expression data using real-time quantitative PCR and the 2-ΔΔct methods. *Methods* **25**, 402.
11 Yang S, Lin G, Tan YQ, Zhou D, Deng LY, Cheng DH *et al.* (2008) Tumor progression of culture-adapted human embryonic stem cells during long-term culture. *Genes Chromosomes Cancer*, **47**, 665–679.
12 Buzzard JJ, Gough NM, Crook JM, Colman A (2004) Karyotype of human ES cells during extended culture. *Nat. Biotechnol.* **22**, 381–382, author reply 382.

13 Imreh MP, Gertow K, Cedervall J, Unger C, Holmberg K, Szöke K *et al.* (2006) In vitro culture conditions favoring selection of chromosomal abnormalities in human ES cells. *J. Cell. Biochem.* **99**, 508–516.
14 Inzunza J, Sahlén S, Holmberg K, Strömberg AM, Teerijoki H, Blennow E *et al.* (2004) Comparative genomic hybridization and karyotyping of human embryonic stem cells reveals the occurrence of an isodicentric X chromosome after long-term cultivation. *Mol. Hum. Reprod.* **10**, 461–466.
15 Hoffman LM, Carpenter MK (2005) Characterization and culture of human embryonic stem cells. *Nat. Biotechnol.* **23**, 699–708.
16 Andrews PW (2002) From teratocarcinomas to embryonic stem cells. *Philos. Trans. R. Soc. Lond.* **357**, 405–417.
17 Sandberg AA, Meloni AM, Suijkerbuijk RF (1999) Reviews of chromosome studies in urological tumors III. Cytogenetics and genes in testicular tumors. *J. Urol.* **155**, 1531–1556.
18 Maitra A, Arking DE, Shivapurkar N, Ikeda M, Stastny V, Kassauei K *et al.* (2005) Genomic alterations in cultured human embryonic stem cells. *Nat. Genet.* **37**, 1099–1103.
19 Longo L, Bygrave A, Grosveld FG, Pandolfi PP (1997) The chromosome make-up of mouse embryonic stem cells is predictive of somatic and germ cell chimaerism. *Transgenic Res.* **6**, 321–328.
20 Wernig M, Meissner A, Foreman R, Brambrink T, Ku M, Hochedlinger K *et al.* (2007) In vitro reprogramming of fibroblasts into a pluripotent ES-cell-like state. *Nature* **448**, 318–324.
21 Houghton FD, Thompson JG, Kennedy CJ, Leese HJ (1996) Oxygen consumption and energy metabolism of the early mouse embryo. *Mol. Reprod. Dev.* **44**, 476–485.
22 Martin KL (2000) Nutritional and metabolic requirements of early cleavage stage embryos and blastocysts. *Hum. Fertil.* **3**, 247–254.
23 Skotheim RI, Lothe RA (2003) The testicular germ cell tumour genome. *APMIS* **111**, 136–150, discussion 150–151.
24 Peter M, Herskowitz I (1994) Joining the complex: cyclin-dependent kinase inhibitory proteins and the cell cycle. *Cell* **21**, 181–184.
25 Gorgoulis VG, Vassiliou LV, Karakaidos P, Zacharatos P, Kotsinas A, Liloglou T *et al.* (2005) Activation of the DNA damage checkpoint and genomic instability in human precancerous lesions Nature. *Nature* **434**, 907–913.
26 Nevins JR (2001) The Rb/E2F pathway and cancer. *Hum. Mol. Genet.* **10**, 699–703.
27 Mahendra R (2004) Conserved and divergent paths that regulate self-renewal in mouse and human embryonic stem cells. *Dev. Biol.* **275**, 269–286.
28 Qin H, Yu T, Qing T, Liu Y, Zhao Y, Cai J *et al.* (2007) Regulation of apoptosis and differentiation by p53 in human embryonic stem cells. *J. Biol. Chem.* **282**, 5842–5852.
29 Lin T, Chao C, Saito S, Mazur SJ, Murphy ME, Appella E *et al.* (2005) P53 induces differentiation of mouse embryonic stem cells by suppressing Nanog expression. *Nat. Cell Biol.* **7**, 165–171.
30 Andrews PW (2006) The selfish stem cell. *Nat. Biotechnol.* **24**, 325–326.
31 Keith WN (2004) From stem cells to cancer: balancing immortality and neoplasia. *Oncogene* **23**, 5092–5094.

Supporting Information

Additional Supporting Information may be found in the online version of this article:

Figure S1. Expression of oncogenes in duplication region of *ch*HES-3 cells.

Figure S2. Microarray data of *ch*HES-3 cells with normal and abnormal karyotype. (a) The Affymetrix Scan Image of karyotypically normal *ch*HES-3 cells. (b) Affymetrix Scan Image of karyotypically abnormal *ch*HES-3 cells. (c) Scatter graph of differentiated genes between karyotypically abnormal and normal *ch*HES-3 cells.

Figure S3. Expression of P53 protein and beta-actin in human embryonic fibroblasts, karyotypically normal and abnormal *ch*HES-3 cells.

Table S1. Primers of RT-PCR.

Table S2. Primers for Real-time RT-PCR.

Table S3. The expression changes of cell proliferation-related genes.

Please note: Wiley-Blackwell are not responsible for the content or functionality of any supporting materials supplied by the authors. Any queries (other than missing material) should be directed to the corresponding author for the article.